

# Flow of Dry Foam in a Pipe

M.Divakaran and S.K.Gupta\*

<sup>1</sup>Department of Chemical Engineering, Indian Institute of Science, Bangalore

\*Corresponding author: email id - sanjeev@chemeng.iisc.ernet.in

**Abstract:** Due to the coupling of foam flow with foam generation step, the earlier experimental studies on foam flow have not led to consistent results. An increase in flow rate to obtain  $\Delta P$  vs.  $Q$  data changes the foam under investigation itself. The controlled experiments carried out earlier in our group show that  $\Delta P$  increases with flow rate as  $Q^{2/3}$ , a weaker dependence than that known for laminar flow or core flow on a slip layer on pipe wall. COMSOL was used to simulate fluid flow in the wall region between two deformed bubbles. The detailed simulations accounted for rheological behavior of surfactant loaded interface influenced by the surfactant transport in the bulk and interface. Simulations with fixed slip layer thickness show a linear relationship of  $\Delta P$  with  $Q$ . Increasing the slip layer thickness has significantly reduced the pressure drop for the fixed flow rate. This result further led to the inference of the squeezing action of the bubble on the liquid against the wall, which raises the pressure on the bubble interface. Increasing the flow rate increases this squeezing pressure and, the bubble responds by increasing the slip layer thickness. This in-effect suppresses the  $\Delta P$  dependence on  $Q$ .

**Keywords:** foam flow, CFD, rheology and slip layer.

## 1. Introduction

Liquid foams have wide range of industrial applications as in enhanced oil recovery process, fire extinguishing systems, froth floatation, foam bed reactors and protein separation. Many of these processes involve handling flow of foams in a pipe, hence understanding the rheology of foam flow is imperative in designing such flow systems. Though foam is a two-phase fluid, a dispersion of gas in liquid, the conventional two-phase methods such as Lockhart-Martinelli correlation severely under predicts the pressure drop incurred for the foam flow (Calvert 1990). Foam exhibits complex rheological behavior with the confounding effects of compressibility, shear thinning, yield stress and slip-like behavior at the wall (Hohler 2005). The complex rheology

of foam is in principle attributed to the structure of foam, with highly deformed polyhedral bubbles immobilized in the matrix of thin liquid films.

Researchers have attempted to develop semi-empirical models based on power law constitutive relations to predict the rheology of foams (Gardeiner 1999). A number of experimental studies are reported in the literature in which foam is generated at different flow rates and pressure drop as function of flow rate is measured. But, in such measurements, foam generation at different rates brings simultaneous variations in bubble size and liquid content of foam. This sets a restraint in studying the effect of flow rate alone on the pressure drop. Isolating the foam production step from the pressure drop measurement allows arresting the variation in bubble size and liquid content of the foam at low flow rates. Such experiments carried out earlier in our group shows that the bubbles flow like plug, sliding over a thin layer of liquid accumulated at the pipe wall (Choudhary 2002). The pressure drop measured in these experiments shows a weak dependence on flow rate -  $\Delta P \propto Q^{2/3}$ .

In this work, we present computational fluid dynamics simulation of foam flow using COMSOL MULTIPHYSICS, to understand the mechanism of foam flow exhibiting such a weak dependence of pressure drop on foam flow rate.

## 2. Model Description

At low flow rates, dry foam slides like a plug over thin slip layer of liquid (figure 1). This visualization is used in developing the model. The conditions at the gas-liquid boundary between the moving core and the liquid layer at the wall need to be specified. The first approximation is to consider no-slip between the moving core and the liquid in the slip layer. The momentum balance based on the wall shear stress ( $\tau_w$ ) and the pressure forces yields the following.

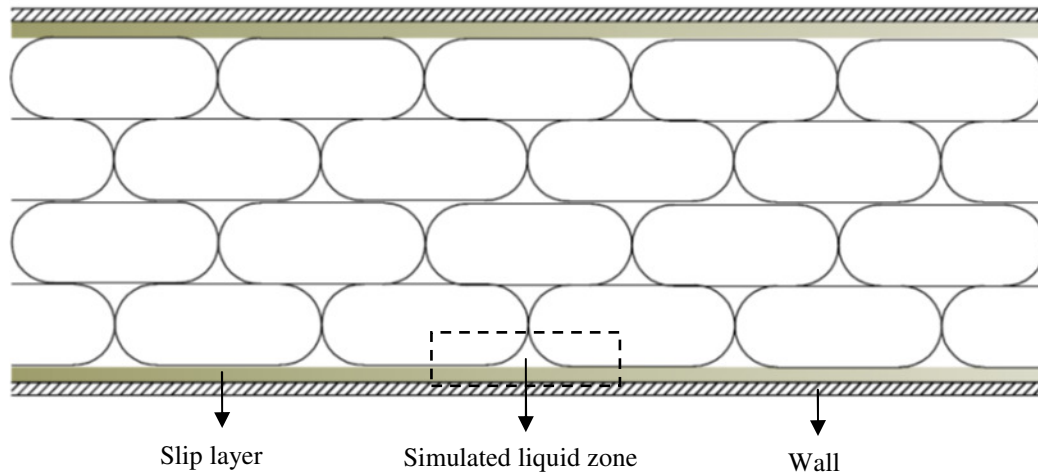


**Figure 1:** Region of simulation

$$\Delta p \pi R^2 = \tau_w 2\pi RL$$

For a wall slip layer thickness of  $\delta$ , the shear stress is calculated from the foam flow rate ( $Q$ ) as:

$$\tau_w = \mu \frac{(Q/\pi R^2)}{\delta}$$

The above equations predict a linear dependence of pressure drop on flow rate, quite different from the weaker dependence observed in the experiments. Moreover, this plug flow model with no-slip between foam core and slip layer over predicts the pressure drop by a factor of ten. If the core-slip layer interface is considered as free surface, the model predicts zero pressure drop as there is no velocity gradient.

To improve model predictions, a more realistic boundary condition, which captures hydrodynamics of the gas-liquid interface realistically, is required. In our model, the flow field in the liquid between two gas bubbles and wall is simulated along with the surfactant transport on the interface. Laminar flow physics module is coupled with transport of dilute species module of COMSOL. The region considered for simulation is shown in Figure 1.

For dry foam, the liquid content is less than 1% and the wall slip layer thickness is in the range of tens of microns.

For dry foam, the liquid content is less than 1% and the wall slip layer thickness is in the range of tens of microns.

Under this condition of low liquid volume fraction at the wall, the domain considered for simulation could be approximated as two-dimensional geometry. The simplified computational domain considered for simulations is presented in Figure 2.

## 2.1 Governing equations and boundary conditions

The Navier-Stokes equation and the surfactant transport equation are solved in the bulk. Sodium dodecyl sulphate is used as a surfactant in the experiments. The surfactant is transported through diffusion and convection in the bulk and gets adsorbed on the interface. The surfactant adsorption process on the interface is assumed to be diffusion controlled. Langmuir adsorption isotherm is used to relate local surfactant concentration on the interface with the bulk concentration near the interface.

The surfactant adsorbed on the interface undergoes surface diffusion and convection on the interface due to the non-zero velocity of the interface. The surfactant balance on the interface forms the boundary condition for solving the surfactant transport in the bulk.

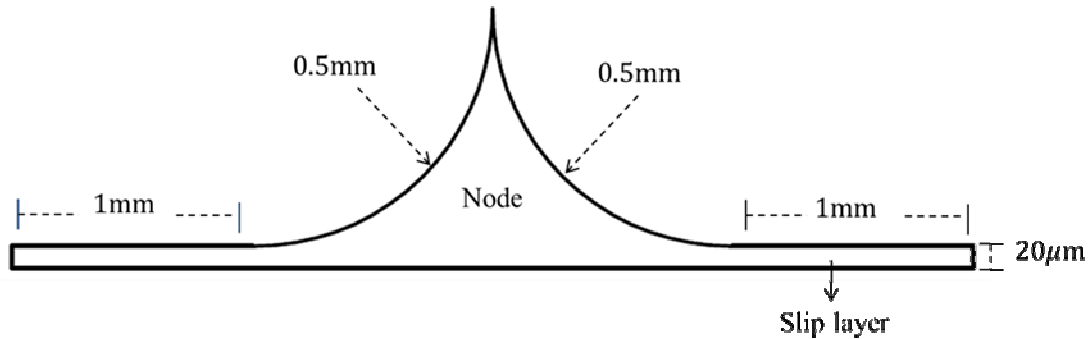


Figure 2: The computational domain

Interface boundary condition for surfactant transport:

$$\nabla_s \cdot (v^s C^s) + \nabla_s \cdot (j^s) = n \cdot j^b$$

The momentum balance on the interface takes into account the interfacial shear stresses and interfacial dilatational stress. In-addition, the surfactant concentration gradient on the interface sets up interfacial tension gradient, termed as Marangoni stresses, which is also accounted in the simulation by coupling surfactant transport with momentum balance. These interfacial rheological processes are incorporated in the simulation through the tangential stress continuity boundary condition on the interface (Edwards 1991, Scriven 1960).

Interface boundary condition for momentum balance:

$$(n \cdot \tau_t) - [(n \cdot \tau_t) \cdot n]n = \nabla_s \sigma + (\mu^s + \mu^d) \nabla_s \nabla_s \cdot v^s$$

The left hand side of the above equation represents the tangential stress exerted on the interface due to velocity gradients in the adjacent bulk liquid. The right side of the equation represents Marangoni stress and the surface viscous stress due to the relative motion among the fluid elements on the interface. A moving frame of reference located on the bubble center is used. The bubble remains stationary and the wall moves relative to it.

### 3. Results and Discussion

Figure 3 shows the velocity field in the new frame of reference. The fluid near the pipe wall picks up momentum from the moving wall and moves along the flow direction. The moving fluid encounters the curved interface of the bubble in front and stagnates there. The pressure rise in the stagnation zone causes the streamlines to turn and generate a vortex in the node region.

The surfactant concentration profile induced by vortex like flow is shown in Figure 4. The stretching and contraction of the interface causes surfactant to deplete or accumulate on the interface. Due to the contraction of the right side interface (Figure 4), under the action of the vortex, the surfactant accumulates on the interface, desorbs and diffuses back to the bulk. The left side interface undergoes stretching motion, which depletes the surfactant on the interface, which in turn sets up diffusion from the bulk to the interface.

The contraction and stretching of the interface creates surfactant concentration gradient along the interface, hence the interfacial tension gradient, also known as Marangoni stress. The interface resists its deformation by the virtue of surface shear viscosity and surface dilatational viscosity. The surface stresses act to immobilize bulk liquid adjacent to them, thereby shearing the liquid and setting up stresses on the wall.

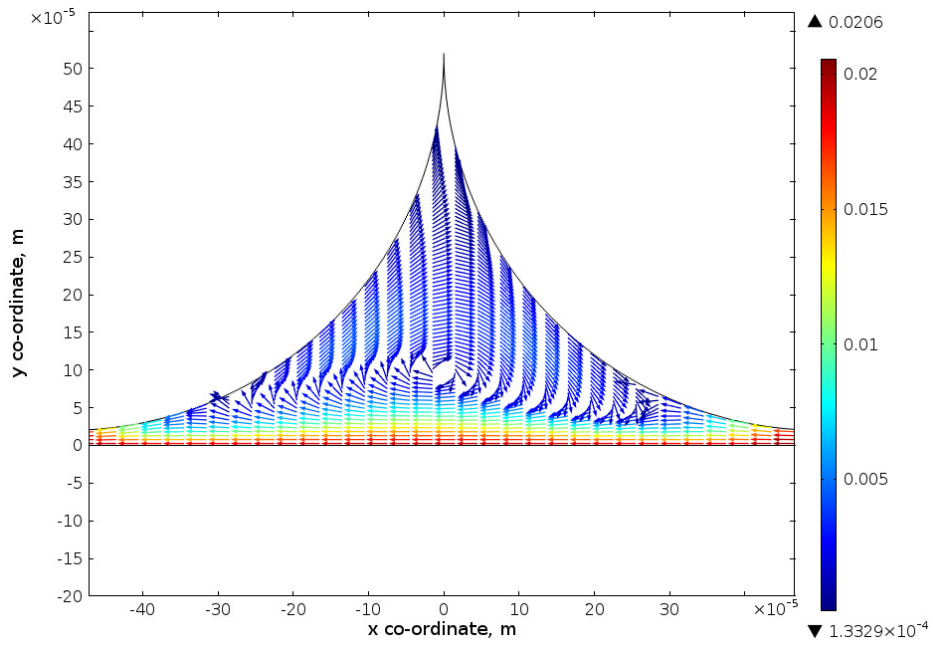


**Figure 3:** Velocity field, (m/s)

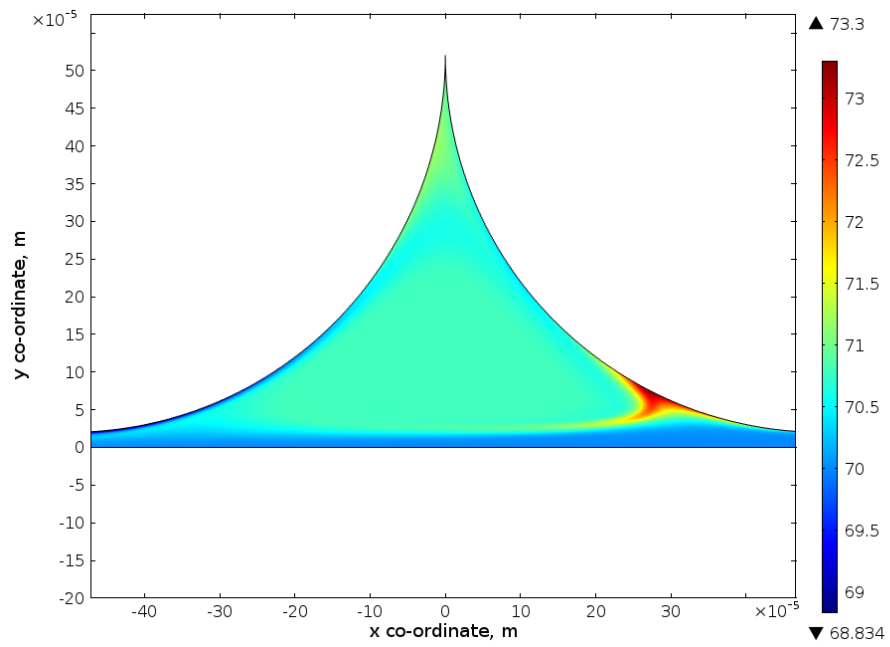


**Figure 4:** Surfactant concentration

The wall shear stress is shown in the Figure 5. The figure shows that shear stresses are generated mostly under the curved region next to the flat portion of the interface. Interestingly, there is no significant stress generated in the portion of the slip layer under flat interface.

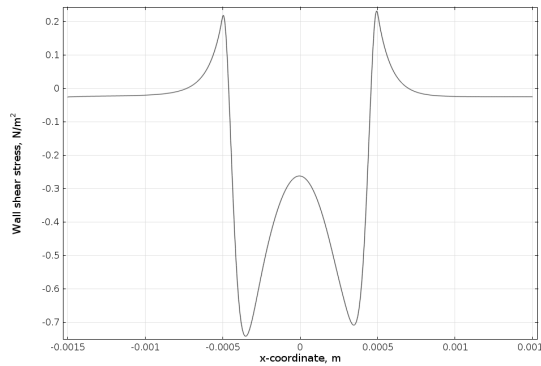


Figure 5: Wall shear stress, N/m<sup>2</sup>

Pressure drop is calculated from the wall shear stress by making the stress balance in the control volume,  $\Delta p \pi R^2 = \tau_w 2\pi RL$ . The wall velocity is varied in the simulations and the pressure drop vs. flow rate trend is produced (Figure 6). The pressure drop vs. flow rate trend shows almost a linear relationship. The exponent of the flow rate in pressure drop relation is about 0.96 for the surfactant concentration well above the critical micelle concentration. These simulations with fixed size of domain and fixed thickness of the slip layer do not lead to a prediction of the experimentally observed weak dependence of pressure drop on flow rate.

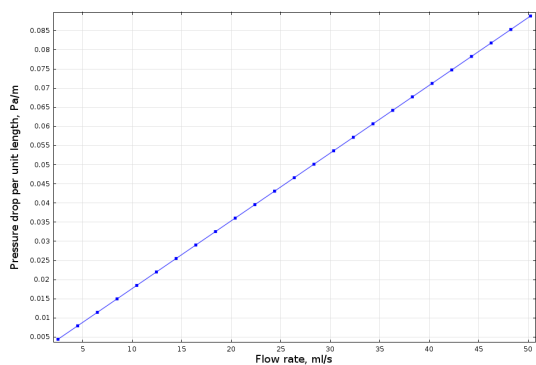


Figure 6: Pressure drop vs. flow rate

An increase in the thickness of the slip layer, due to the negligible shear stress on the wall in the flat region, is expected to play an insignificant role in affecting the pressure drop. The model prediction however shows quite the opposite. An increasing the slip layer thickness significantly reduces the pressure drop. Figure 7 shows static pressure along the interface for two different slip layer thicknesses. The peaks in the pressure profile correspond to zone where the bubble tends to squeeze the liquid against the wall as it moves forward. With an increase in the slip layer thickness, the pressure required for the bubble to squeeze the liquid decreases as shown in Figure 7.

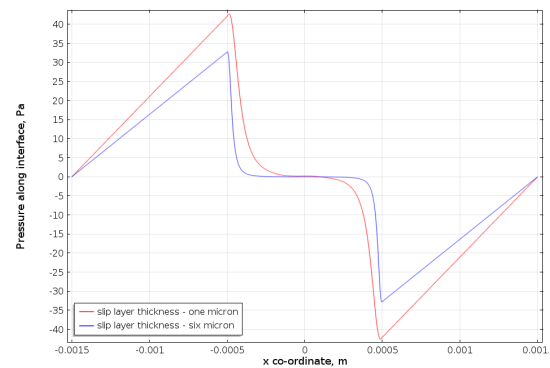


Figure 7: Pressure along the interface

#### 4 Conclusions

The simulation results for fixed slip layer thickness show that the computed pressure drop receives no contribution from the region where the bubble surface is parallel to the wall (flat region). An increase in film thickness, which is varied in the range of tens of microns, however decreases the pressure drop sensitively. The dominant contribution to pressure drop comes from the liquid being squeezed under an advancing bubble. An increase in foam velocity increases the pressure under the advancing bubble, which, due to the deformable shape of bubble, is expected to increase the thickness of the slip layer left behind. The increased slip layer thickness at increased flow rate, in agreement with the experimental observations (Thondavadi 1985), requires less squeezing of liquid under the advancing bubble and therefore the weakened dependence of  $\Delta P$  on  $Q$ .

## 5. References

Calvert, J. R. (1990). Pressure drop for foam flow through pipes. *International Journal of Heat and Fluid Flow*, 11(3), 236-241.

Choudhary, H. (2002) Experimental Investigations on foam flow. Master's thesis, Chemical Engineering, Indian Institute of Science, Bangalore.

Edwards, D.A., Brenner, H. and Wasan, D.T. (1991) *Interfacial Transport Processes and Rheology*. Butterwoth Heinemann.

Gardiner, B. S., Dlugogorski, B. Z., & Jameson, G. J. (1999). Prediction of pressure losses in pipe flow of aqueous foam. *Industrial and Engineering Chemistry Research*, 38(3), 1099-1106.

Hohler, R, & Cohen-Addad, S. (2005). Rheology of liquid foam. *Journal of Physics: Condensed Matter*, 17, R1041-R1069.

Scriven, L.E. (1960). Dynamics of a fluid interface. *Chemical Engineering Science*, 12, 92-108.

Thondavadi, N. N., & Lemlich, R. (1985). Flow properties of foam with and without solid particles. *Ind. Eng. Chem. Process. Dev.*, 74(3), 748-753.

## Notations

|                |   |
|----------------|---|
| Q              | Flow rate, ml/s   |
| L              | Pipe length, m  |
| R              | Pipe radius, m  |
| C              | Surfactant concentration in the bulk, mol/m <sup>3</sup>      |
| C <sub>s</sub> | Surfactant concentration on the interface, mol/m <sup>2</sup> |
| $v^s$          | Interface velocity, m/s                                       |
| $j^s$          | Surfactant flux on the interface, mol/m <sup>2</sup> .s       |
| $j^b$          | Surfactant flux on the interface, mol/m <sup>3</sup> .s       |

## Greek Letters

|            |  |
|------------|--|
| $\Delta p$ | Pressure drop, Pa/m                      |
| $\tau_w$   | Wall shear stress, N/m <sup>2</sup>      |
| $\tau_l$   | Shear stress in liquid, N/m <sup>2</sup> |
| $\sigma$   | Interfacial tension, N/m                 |
| $\nabla_s$ | Surface gradient operator                |
| $\mu^s$    | Surface shear viscosity, Pa.m.s          |
| $\mu^d$    | Surface dilatational viscosity, Pa.m.s   |
| $\delta$   | Slip layer thickness, microns            |